Biocementation for desert sand against wind-induced erosion with different treatment processes

Yang Liu[1,2] · Yaqing Gao[2] · Bin Liu[1,2] · Xinwen Cao[1,2] · Jiawei Chen[1,2]

Abstract

Purpose Wind-induced erosion is a serious problem that yields soil degradation and environmental pollution. Biocementation technologies have shown potential for sand fixation and wind erosion control in deserts and arid regions. The topic of this study is to investigate the effectiveness of biocementation against wind-induced erosion with different treatment processes.
Methods Biocementation was achieved through soybean-urease induced calcium carbonate precipitation. Three different volumes of treatment solution were used to treat sand specimens by spraying, mixing and the combination methods in this study. The characteristics of sprayed and mixed crust were shown, and the properties of all the biotreated specimens including $CaCO_3$ distribution, wind erosion rate, and penetration resistance were measured.
Results The carbonate content in the soil increased with the amount of treatment solution. At the same dosage, the spraying method concentrated 1.0%-1.4% $CaCO_3$ in the surface soil, while the mixing method generated 0.8% $CaCO_3$ in a uniform spatial distribution. The top-concentrated $CaCO_3$ resulted in a lower initial wind erosion rate of the sprayed specimen. The overall reinforcement of the soil by the mixing method produced higher penetration resistance and inhibited the development of wind erosion. The combination of the two methods increased penetration resistance to 200 N and reduced the wind erosion rate to almost 0 $g \cdot m^{-2} \cdot min^{-1}$.
Conclusion The spraying and mixing methods induced different distribution patterns of $CaCO_3$ precipitations in soil, leading to varying biocementation effectiveness. To resist severe and continuous wind-induced erosion, a combination of the two methods can be considered to improve the uniformity and strength of biocementation within a certain depth of the soil.

Keywords Soybean-urease induced carbonate precipitation · Biocementation · Treatment method · Wind erosion rate · $CaCO_3$ distribution · Penetration resistance

1 Introduction

Wind erosion is a natural process that refers to the displacement of soil particles and the destruction of surface structures with the blowing wind (Kok et al. 2012). It is the first

✉ Yaqing Gao
  gaoyq@hhu.edu.cn

1 Key Laboratory of Ministry of Education for Geomechanics and Embankment Engineering, Hohai University, No.1, Xikang Road, Nanjing 210098, Jiangsu, China

2 College of Civil and Transportation Engineering, Hohai University, No.1, Xikang Road, Nanjing 210098, Jiangsu, China

link of desertification in arid and semi-arid regions. Wind erosion decreases the fine-grained soil particles and the blown dust worsens the air and water quality, posing challenges to agriculture and human health (Xu et al. 2020; Li et al. 2021). Consequently, there is an urgent need to find a practical solution for combating wind erosion. Soil cementation techniques based on microbial or enzymatic processes have attracted increasing attention in the field of sand stabilization and wind erosion control (Almajed et al. 2020b; Fattahi et al. 2020; Sun et al. 2021; He et al. 2023;). During the processes, the hydrolysis of urea is catalyzed by the bacteria or urease enzyme, releasing a large amount of free carbonate ions, which react with free calcium ions in the reaction system to form calcium carbonate precipitations (as described in Eq. 1 and 2). The produced carbonate can interconnect soil particles and fill soil voids, which provides resistance

against movement and deformation by wind force (Dubey et al. 2023). Evidences have been reported that the threshold velocity (i.e., a wind velocity at which soil particles start to move) of desert sand can be increased from 20 km/h to 45–55 km/h after biocementation treatment (Dubey et al. 2021; Liu et al. 2023b).

$$CO(NH_2)_2 + 2H_2O \xrightarrow{\text{Urease}} 2NH_4^+ + CO_3^{2-} \tag{1}$$

$$Ca^{2+} + CO_3^{2-} \rightarrow CaCO_3(s) \tag{2}$$

Homogeneous cementation is a key to biotechnology, especially for large-area applications. The method of introducing the biotreatment solution into soil largely determines the spatial distribution of calcium carbonate precipitations (Almajed et al. 2018; Ossai et al. 2020; Alwalan et al. 2023). It has been reported that an inappropriate treatment tends to increase the risk of bioclogging, form uneven carbonate precipitations and weaken soil strength (Mujah et al. 2017). Previous studies have commonly used spraying and mixing methods for surface erosion control (Wang et al. 2024). The spraying method evenly sprays the treatment solution onto the soil surface (Hamdan and Kavazanjian 2016; Zomorodian et al. 2019; Chung et al. 2021). During treatment, surface soil is the first to contact the treatment solution and gains surface strength efficiently, making the spraying method particularly suitable for wind erosion control. It has little disturbance to the site and is the most convenient method applicable for field test (Meng et al. 2021). However, the interior of the soil remains inadequately cemented, which is still at the risk of erosion under continuous wind erosion (Liu et al. 2023a). Mixing method mixes the soil with the treatment solution and compacts it to the desired density. The treatment range is artificially controlled and a more uniform cementation along the depth can be achieved (Sharaky et al. 2018; Almajed et al. 2020b). Zuniga-Barra et al. (2023) used mixing method for adding biocement reagents into tailing deposits to control dust emission. They found that mechanical mixing improved the surface strength of the biocemented material. However, the mixing treatment of biocementation for wind erosion resistance has not received much attention.

The results of previous studies differ in biocementation effectiveness and the most efficient biotreatment method. The differences may be caused by multiple factors such as the type of urease (Ahenkorah et al. 2020; Liu et al. 2023a), the concentration of the treatment solution (Liu et al. 2023b), the type of tested soil (Almajed et al. 2020a) and the method of specimen preparation (Alwalan et al. 2023). Comparison between various biotreatment methods was seldom carried out under similar test conditions. In addition, available studies used different methods to estimate wind erosion resistance, including the wind erosion rate/amount (defined as the amount of soil loss per unit area over a certain period of time) (Maleki et al. 2016; Almajed et al. 2020b; Gao et al. 2022) and the threshold detachment velocity (defined as the critical wind speed at which the soil loss begins to occur) (Hamdan and Kavazanjian 2016; Woolley et al. 2020). Some other parameters are also used to evaluate the wind erosion resistance, such as surface penetration force/strength (Rice et al. 1997; Maleki et al. 2016; Almajed et al. 2020b), $CaCO_3$ content (Fattahi et al. 2020; Dubey et al. 2021; Liu et al. 2023a), PM 2.5/10 (Song et al. 2020) and so on. The indicators above represent various physical dimensions such as mass, velocity, force, etc., making it challenging to compare them with each other. Only Baziar et al. (2021) tested the amount of soil loss of biocemented sand by spraying and mixing methods under consistent experimental conditions. However, they just verified the effectiveness of the two methods without reporting their discrepancy. Therefore, it is necessary to conduct more experiments under consistent experimental conditions and same evaluation methods to study the effect of biotreatment methods on wind erosion control.

The objective of this study is to investigate the effect of treatment methods on wind erosion resistance of desert sand. Considering environmental friendliness and low-cost, soybean-urease induced carbonate precipitation (SICP) technology was employed to stabilize the desert sand. Spraying, mixing and the combination of the two methods were used to prepare sand specimens with varying treatment dosage. To determine the effectiveness of various treatment methods, the erosion rate induced by the continuous wind force with impacting particles, the crust thickness and the penetration force were measured. The spatial distribution and microscopic characteristics of carbonate precipitations were analyzed to explain the differences between the spraying and mixing treatment. The advantages of the combined method in resisting wind erosion were confirmed in the comparison.

2 Materials and methods

2.1 Materials

In this study, the crude soybean urease was extracted by dissolving soybean powder (< 0.15 mm) in deionized water, filtering and centrifuging (Gao et al. 2019). The concentration of dissolved soybean powder was 40 g·L^{-1}. The electrical conductivity (EC) method (Whiffin et al. 2007) was adopted for urease activity measurement. At room temperature (25°C), the activity of soybean urease was about 5.33 mmol·L^{-1}·min^{-1}. Equal mole of $CaCl_2$ and urea were used as cementation solution, providing the enzymatic reactants and calcium sources in the reaction. All the chemicals

were reagent grade with a purity of 99%, and the concentration of them was 0.6 mol·L^{-1}.

The desert sand used was collected from the southeast edge of the Tengger Desert in Shapotou, Ningxia, China. The specific physical parameters of desert sand and detailed test methods are shown in Fig. S1 and Table S1 in the Supplementary Material.

2.2 Sand specimen treatment

The treatment program is summarized in Table 1 and the treatment process is shown in Fig. 1. All tests were triplicated for repeatability. Specimens were prepared in stainless-steel pans (24×17×4 cm) with small holes (5 mm in diameter) at the bottom for allowing drainage, where a layer of 300-mesh nylon filter paper was attached to prevent the loss of sand.

Spraying method for specimen treatment was taken by the following steps (adapted from Liu et al. 2023b): (1) sieving (0.2 mm) and filling the desert sand in the pans to a density of 1.51 g·cm^{-3}; (2) preparing SICP solution by mixing the soybean urease solution and cementation solution in equal volumes; (3) spraying the SICP solution onto the surface of specimens evenly and incubating the specimens at room temperature for 48 h; and (4) rinsing

the specimens with 3 times the pore volume of deionized water to remove the soluble substances, then oven-drying at 60℃.

The mixed specimens were prepared by mixing the SICP solution with pre-weighed desert sand and subsequently filling it in the pans. Specific treatment steps are as follows: (1) weighing a certain mass of sieved desert sand (according to the dry density of 1.51 g·cm^{-3}) and mixing it with the prepared SICP solution; (2) dividing the mixed samples into three equal parts, filling each part in the pan and compacting them to a certain height; (3) trimming the sand surface with a steel ruler to match the same height of the pan, then incubating the specimens at room temperature for 48 h; (4) rinsing the specimens with 3 times the pore volume of deionized water to remove the soluble substances, then oven-drying at 60℃.

Three groups of specimens were treated by the combination of mixing and spraying. The treatment solution and desert sand were first homogenized using the mixing method described above. After 24 h of mixing treatment, an equal amount of the treatment solution was then uniformly sprayed onto the sand surface. The specimens were also allowed to wait for complete cementation, then rinsed and dried for subsequent tests. It should be noted that the same total amount of treatment solution was used

Table 1 Treatment program for desert sand

Specimen number	Treatment method	Amount of SICP solution	Treatment range (in depth, cm)
S1	Spraying	2 L·m^{-2}	
S2		4 L·m^{-2}	
S3		6 L·m^{-2}	
M1	Mixing	60 mL	4
M2		120 mL	
M3		180 mL	
C1	Combination (mixing & spraying)	60 mL + 2 L·m^{-2}	4
C2		120 mL + 4 L·m^{-2}	
C3		180 mL + 6 L·m^{-2}	

Fig. 1 The processing diagram of specimen treatment
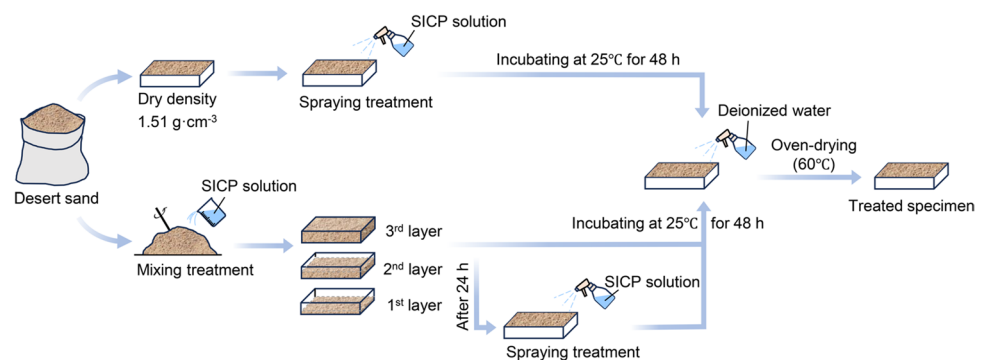
for specimens S2, M2, and C1 in Table 1, which will be compared in the Results.

2.3 Wind erosion test

The wind erosion device in Liu et al. (2023b) was used to conduct wind erosion test on SICP-treated specimens. The wind erodibility of each specimen was measured at a wind velocity of 10 m·s^{-1} under the impacts of wind-blown sand particles for up to 30 min. The tested wind velocity was chosen based on historical wind scales in Shapotou area (excluding chance events on very few days) (as shown in Fig. S2 in the Supplementary Material), and it was calibrated using an anemometer (Smart Sensor AS386). To simulate the impacting particles, the desert sand was steadily provided through a sand feeder at a rate of 3.18 g·s^{-1}, which was calculated according to Bagnold's sand transport theory (Bagnold 1941). Before the test, each specimen was weighed using an electronic scale (accuracy 0.01 g) and the initial mass was recorded. The specimens were weighed every 2 min to calculate the mass loss and converted to wind erosion rate by Eq. 3:

$$E = \frac{\Delta M}{S \cdot t} \tag{3}$$

where E is the wind erosion rate (g·m^{-2}·min^{-1}), ΔM is the mass loss of the eroded specimen (g), S is the surface area of the specimen (cm^2), and t is the wind erosion time (min).

2.4 Penetration test

A micro-penetrometer (HP-50, Aidebao, China) with a flat-bottomed cylindrical probe was adopted to assess the penetration resistance of the SICP-treated specimens. The penetrometer was connected to a computer to automatically record the normal force and displacement applied to the specimen. The cone with a diameter of 6 mm penetrated through the specimen from the surface at a steady rate (about 1 mm·min^{-1}) until the penetration force remained stable. To obtain representative results, at least five undisturbed test points were taken on each specimen.

2.5 Other tests

The shear strength behavior of the untreated and SICP-treated sand specimens was investigated. Due to limitations in sampling size and soil homogeneity, only specimen M3 was tested to verify the improvement of soil mechanical properties by SICP treatment. The test was conducted using a strain-controlled direct shear device (model ZJ-1A), following ASTM D3080 (ASTM 2012). Soil samples were cut using a ring cutter (61.8 mm in diameter, 20 mm in height) and then sheared at vertical pressures of 100, 200, 300, and 400 kPa and a shear rate of 1 mm·min^{-1}. The untreated sand was directly filled in the shear box at a density of 1.51 g·cm^{-3} for testing.

About 5 g sand sample was taken from the top and bottom of the crust to measure the CaCO$_3$ content. The soil at the bottom of the sprayed specimens was also measured. The samples were placed in 10 mL of 1 mol/L hydrochloric acid to dissolve the CaCO$_3$. The concentration of the aqueous calcium in the hydrochloric acid was measured using the EDTA titrimetric method (ISO 1984).

To characterize the bonding behavior between the CaCO$_3$ crystals and sand particles, scanning electron microscopy (SEM) analysis was conducted on the small pieces of cemented sands, which were cut from the surface layer of specimens. The SEM tests were performed using Sigma 300, ZEISS, Germany.

3 Results

3.1 Apparent characteristics of SICP-cemented crust

Dummy Fig. 2 shows the photographs of crusts taken from sprayed and mixed specimens. It can be seen that the thickness of the sprayed crust increased with the increasing spray volume. When the spray volume increased from 2 L·m^{-2} to 6 L·m^{-2}, the thickness of the crust thickened from 0.8 cm to 2 cm accordingly. In addition, it can be observed that the bottom of the sprayed crust is uneven and some weakly cemented sand particles detached from the bottom during sampling. In contrast, the thickness of the mixed crusts reached approximately 3 cm regardless of dosage. The strength of the mixed specimens improved with increasing mixing volume, as evidenced by a fragile crust at low dosage (Fig. 2d), and a hard crust at high dosage (Fig. 2e and f). At the same time, the appearance of the crusts was more complete, indicating that the mixing method allowed for uniform cementation over the target treatment range.

3.2 Mechanism of SICP against wind erosion

Figure 3 presents the distribution of CaCO$_3$ content in the soils. It should be noted that the crust of specimen sprayed with 2 L·m^{-2} solution was too thin to be sampled separately at the top and bottom, so only one data was tested for this group of specimens. For all specimens, the mass of carbonate precipitation in the crust increased with the increasing spraying/mixing volume. At the same volume of treatment solution, the CaCO$_3$ content of the sprayed specimen was significantly higher than that of the mixed specimen. This is since the treatment solution is stored in the top soil layer of sprayed specimens, and artificially dispersed in all the pore space of mixed specimens. For the same reason, the

Fig. 2 The crusts of SICP-treated specimens: **a-c** formed by spraying method; **d-f** formed by mixing method
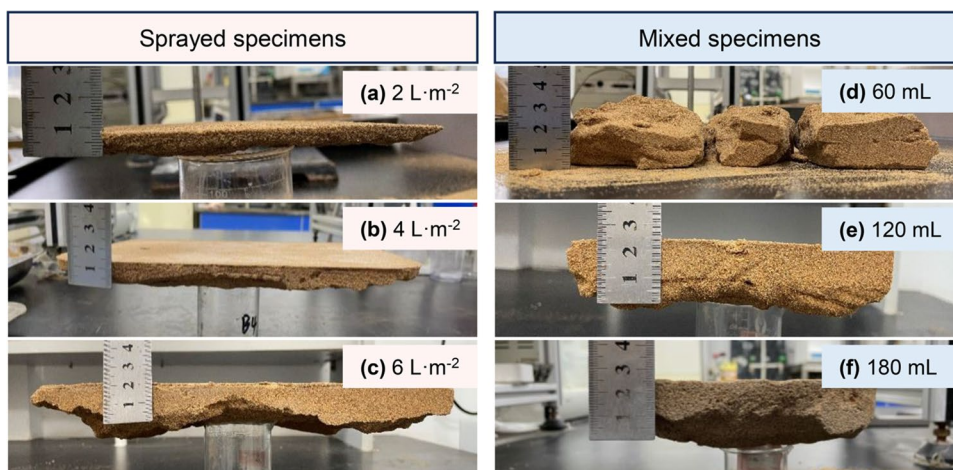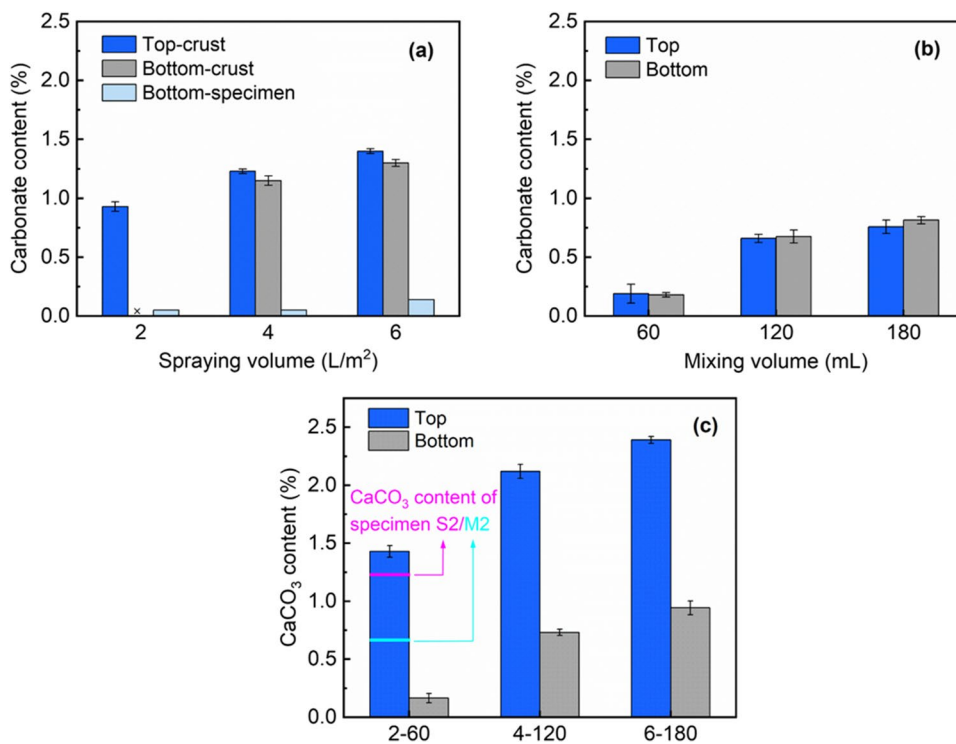

Fig. 3 The CaCO₃ precipitation distribution by different treatment methods: **a** spraying; **b** mixing; **c** combination

CaCO₃ content at the top of the sprayed crust was much higher than that at the bottom, whereas the calcium carbonate precipitations in the mixed crusts showed a homogeneous distribution. Occasionally, under the effects of gravity and layered compaction, some of treatment solution in the upper soil layer could be pressed into the lower soil layer, resulting in higher content at the bottom of specimens. For the specimens treated using combination method, specimen 2–60 was compared with specimen S2 (treated with a spray volume of 4 L·m^{-2}) and M2 (treated with a mix volume of 120 mL) here, as they both utilizaed the same dosage of SICP solution. It is evident that the CaCO₃ content at the top of the crust was 0.25% higher than that of the spraying

method and 0.75% higher than that of the mixing method. This is attributed to the initially mixing treatment, which filled some of the soil pores with carbonate precipitations, thereby reducing the permeability of soil. Consequently, the subsequently sprayed SICP solution was held in the upper soil, leading to a notable increase in CaCO₃ content.

According to the above comparisons, the cementation depth of the mixed specimen depends on the sample preparation (i.e., artificial influence) and the cementation level is proportional to the amount of treatment solution. In contrast, the cementation depth of the sprayed specimen is proportional to the amount of treatment solution, and the cementation level decreases with depth. The combined treatment of

mixing and spraying both increases the calcium carbonate content at the top and the bottom soil, which benefits the overall resistance of wind erosion.

The microscopic characteristics of sprayed and mixed crusts were observed, and the SEM images of specimens S3 and M3 were presented in Fig. 4. Observations showed that the CaCO$_3$ crystals generated by spraying method were mostly distributed between adjacent particles. The crystals were stacked to form clusters with a regular spherical shape. The diameter of individual spherical clusters was about 4–6 μm, and there were also a few small crystals with a size of less than 1 μm. In contrast, the calcium carbonate crystals precipitated by the mixing method more densely cover the particle surface. The crystals were smaller in size (less than 3 μm) and more numerous but did not form regular clusters. It is speculated that the mixing process caused external damage to the connections between the calcium carbonate crystals. Lin et al. (2016) categorized the CaCO$_3$ precipitation patterns into three types, including contact-cementing, particle-coating and matrix-supporting. It is generally recognized that the contact-cementing has higher stabilization efficiency (Hoang et al. 2019; Zhang et al. 2021). For the particle-coating precipitations, they may contribute more to filling the matrix and increasing the bearing capacity.

Carbonate precipitation was found to produce interfacial bond strength with silica through nonbonded interactions and diffusing into the crystal structure of the substrates (Ghasemi et al. 2022). The results of the direct shear test in Fig. 5 show a significant increase in cohesion (i.e., the intercept of the fitted line) after the SICP treatment, from 5.960 kPa to 13.775 kPa, and a slight increase in friction angle (i.e., the slope of the fitted line), from 30.1° to 31.0°. The increasing cohesion induced by biocementation can
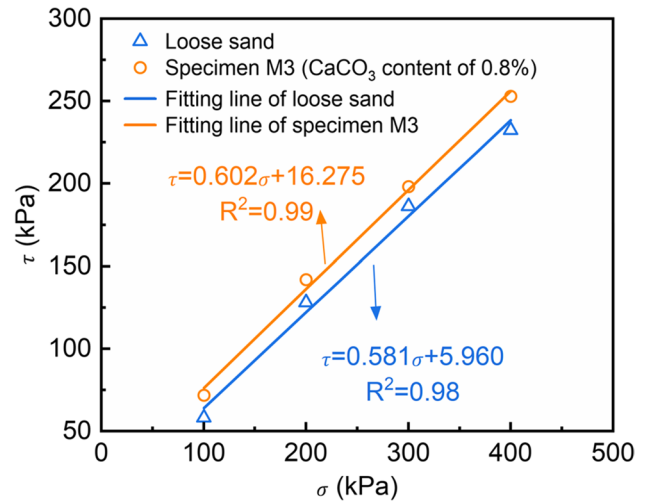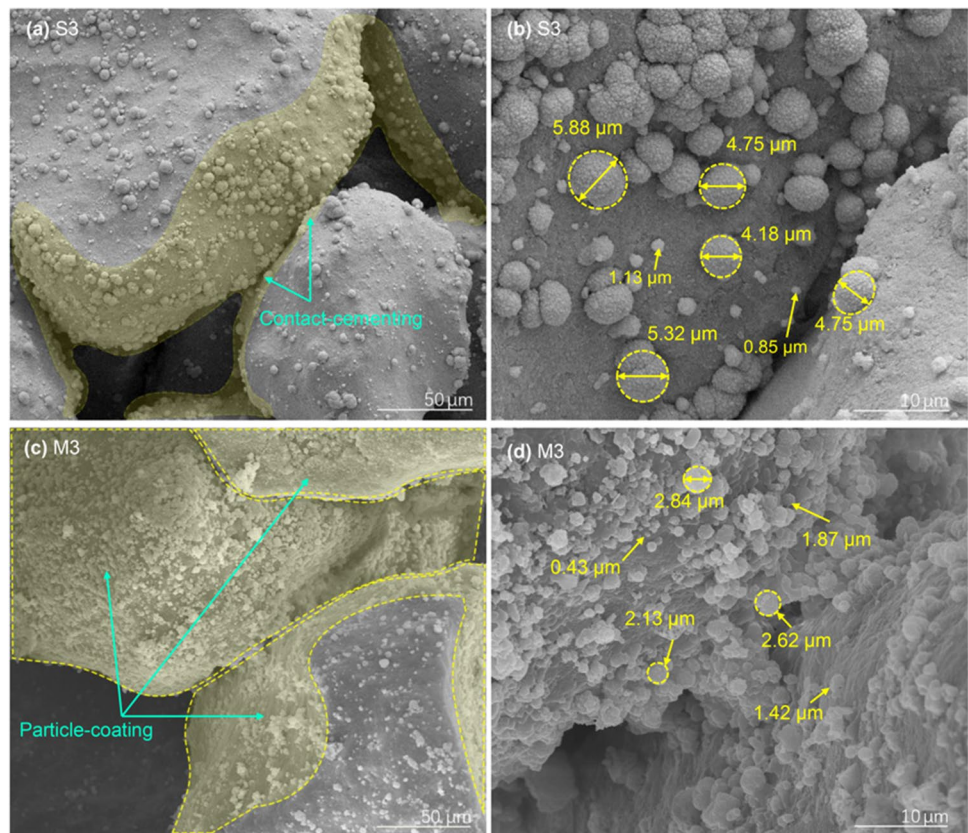

Fig. 5 Enhancement of cohesion in desert sand after SICP treatment

Fig. 4 SEM images of the cemented crust: a-b specimen S3 by spraying treatment; c-d specimen M3 by mixing treatment
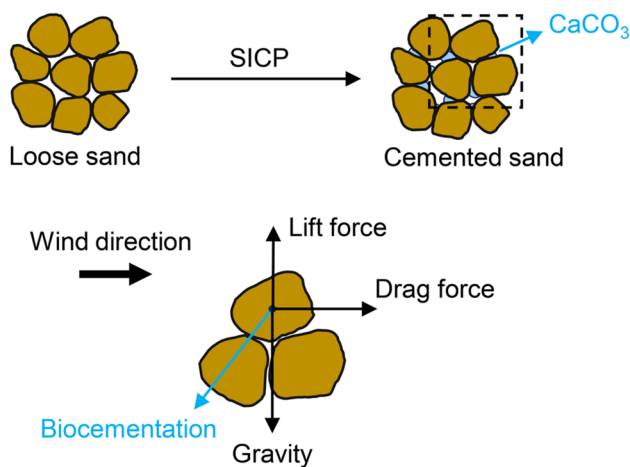
Fig. 6 Schematic diagram of the mechanism of SICP technology against wind erosion

Fig. 7 The broken crust and the hollowing out of inner sand

withstand the lifting and dragging forces of wind on the soil particles, thereby impeding particle movement and controlling wind erosion (Fig. 6). Moreover, the separate sand particles are bonded together by the calcium carbonate to form agglomerates of greater diameter and mass to keep stable.

3.3 Wind erosion rate

Figure 7 shows an eroded sprayed specimen, where the scratches left on the surface by the impacting particles and the breakdown of the crust can be observed. With the SICP treatment, the upper desert sand is cemented into a hard crust to resist wind erosion. Once the crust breaks down, the loose sand under the crust layer will be rapidly blown away, causing a sharp increase in the wind erosion rate. It

can be hypothesized that a thicker crust can slow down the development of wind erosion.

The results of wind erosion rate are shown in Fig. 8. The S1 specimen (with a spray volume of $2 L \cdot m^{-2}$) has a certain wind erosion rate at the beginning of the test, indicating that the threshold velocity is lower than 10 m/s. The wind erosion rate increases slightly in the first 5 min. When the wind erosion lasted for about 10 min, the crust was damaged and the uncemented sand under the crust was gradually exposed to erosion, resulting in an exponential increase in wind erosion rate. Until the end of the test, the wind erosion rate of S1 exceeded $5000 g \cdot m^{-2} \cdot min^{-1}$, indicating that the specimen has completely lost the resistance to wind erosion. The wind erosion rate of the S2 specimen (with a spray volume of 4 $L \cdot m^{-2}$) was kept at $0 g \cdot m^{-2} \cdot min^{-1}$ at the beginning because the threshold velocity is higher than 10 m/s. Thereafter, under the impact of wind and sand particles for 12 min, the crust of the specimen gradually broke and the wind erosion rate began to increase over time. The change in wind erosion rate with time for the S3 specimen (with a spray volume of 6 $L \cdot m^{-2}$) followed the same pattern as that of the S2 specimen, which began to show mass loss after 15 min. Since the crust of S3 was thicker than that of S2, the internal uncemented sand was exposed later, leading to a lower erosion rate of S3 at the same time. However, it is envisioned that both S2 and S3 specimens will show an exponential increase in erosion rate under longer or more severe wind erosion, as similar to specimen S1.

The wind erosion rate with time of the mixed specimen is different from that of the sprayed specimen. It can be seen from Fig. 8b that, the wind erosion rate of the mixed specimens remained relatively stable over time within a certain range, which is attributed to the overall cementation. Even if the surface soil is blown away, the inner sand remains resistant to wind erosion. At various mixing volumes, the cementation level of the specimens increased with the increasing mixing volume, and the wind erosion rate decreased. Comparing the wind erosion rates of the sprayed and mixed specimens, it can be found that the sprayed specimens can keep non-eroded for a while at a high volume of treatment solution, whereas the mixed specimens always have a certain wind erosion rate immediately at the beginning of the erosion. This agrees with the distribution of calcium carbonate precipitations in soil, which is concentrated with higher content in the surface crust of the sprayed specimens and uniformly dispersed with lower content in the mixed specimens. As a result, the mixed specimens continue to be eroded over 20 min, accumulating a large total mass loss.

The wind erosion rate in Fig. 8c is generally as expected for combined treatment. It can be seen that the specimen 2–60 was eroded and the erosion rate still tended to increase with time. At the end of the test, the wind erosion rate was $400–500 g \cdot m^{-2} \cdot min^{-1}$. However, this value was greatly

Fig. 8 Different growth patterns of wind erosion rate curves: **a** exponential for spraying method; **b** constant for mixing method; **c** significant reduction for combination method
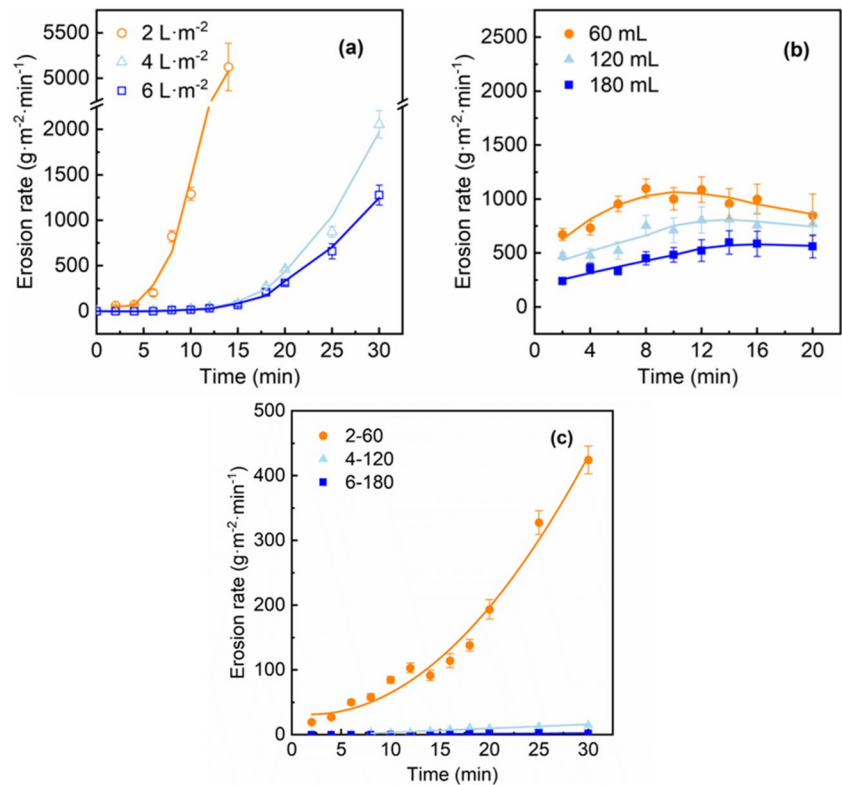
reduced compared to the mixed specimen. The increase in wind erosion rate with time was also reduced as compared to the sprayed specimen, suggesting a slowing down of the breakage of the crust. At higher cementation levels, specimen 4–120 and 6–180 hardly produced mass loss in the experiment. These results directly demonstrate that the combination treatment of mixing and spraying further improves the wind erosion resistance of desert sand and extends the effective period.

3.4 Penetration resistance

The penetration curves of all specimens are shown in Fig. 9. It can be seen that the maximum penetration force always increases with the increasing treatment dosage, benefiting from more carbonate precipitations and higher cementation level. At the same treatment dosage, the combination method has the greatest penetration force and the mixing method has the least penetration force, which also corresponds to the
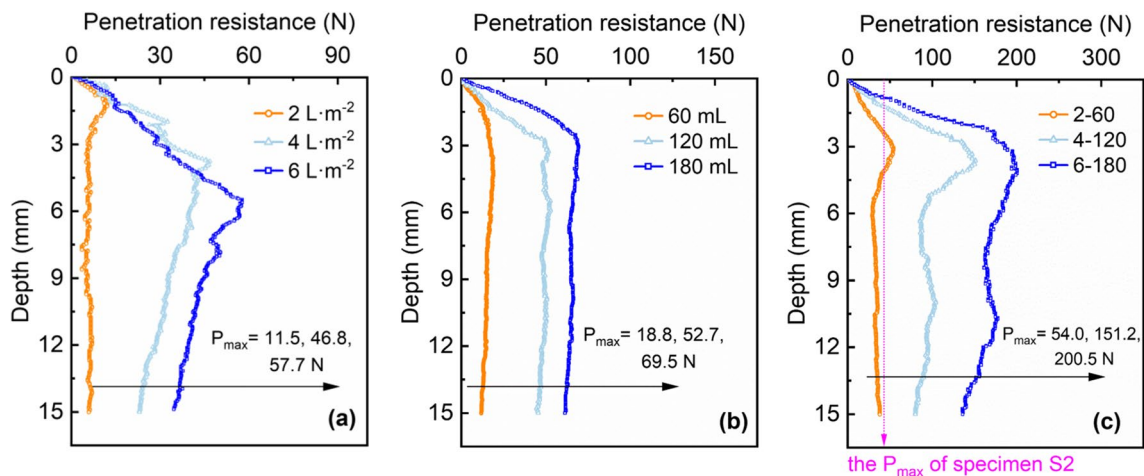

Fig. 9 The penetration curve of specimens by different treatments: **a** spraying method; **b** mixing method; **c** combination method. P_{max} represents the maximum force during penetration. Specimen S2 corresponds to the spraying volume of 4 L·m^{-2}

results of $CaCO_3$ content. In addition, for spraying specimens, the penetration depth corresponding to the maximum penetration force increased (i.e., the peak point of the penetration curve shifts downward in Fig. 9a) with the spray dosage. It can be explained by the layer boundary theory in cone penetration testing (CPT), which means that the penetration resistance exhibits the properties of the underlying soil layer before the cone reaches the soil layer boundary (Ma et al. 2017). In other words, the position of the soil boundary affects the shape of the penetration curve. The thickness of the sprayed crust increased with dosage, resulting in a downward shift of the soil boundary, which is shown on the penetration curve as an increasing depth corresponding to the peak point. In contrast, the mixed specimens formed a uniform cementation that stabilized the peak point at a stable depth. For combined specimens, the peak points were caused by the further spray treatment. However, due to the internal cementation by initial mixing treatment, the depth of the peak points did not change significantly.

4 Discussion

This study verified that the effectiveness of spraying and mixing methods depended on the amount of treatment solution. However, the homogeneity of cementation in soil was different between the two methods at the same volume of treatment solution. In the spraying process, the treatment solution infiltrated from the soil surface to the interior, generating a top-concentrated distribution of $CaCO_3$; the mixing process artificially dispersed the solution in the soil pores, forming a uniform distribution of $CaCO_3$. In other words, the effective stabilization area of the spraying and mixing methods is the surface soil and the internal soil, respectively. This was also confirmed by the thickness and penetration force of the crusts. The spatial distribution of biocementation determines that spraying is suitable for resisting light or short-term strong wind erosion occurring on the soil surface. Once the surface crust is destroyed, the internal unconsolidated sand will be rapidly hollowed out, as indicated by the exponential increase in the erosion rate curve (Liu et al. 2023a). Therefore, it is necessary to deepen the treatment depth to cope with intense and continuous erosion. Increasing the spraying volume is an alternative, but percolation of sand particles could reduce urease activity and precipitation efficiency (Chae et al. 2021; Liu et al. 2024). The mixing method can effectively solve this problem, and the treatment depth is artificially controllable, which is a clear advantage. The combined method can achieve both overall soil stabilization and enhance the wind erosion resistance of the surface soil. By considering the advantages of spraying, mixing and combined methods, as well as controlling the treatment dosage, it is possible to choose the most effective treatment for different degrees of wind erosion. However, an obvious main challenge for mixing treatment is achieving high construction efficiency and low cost, which will be investigated in a subsequent phase of this work.

5 Conclusions

In order to mitigate wind erosion in desert areas, soybean-urease induced calcium carbonate precipitation was used to improve wind erosion resistance of desert sand. The effects of different treatment methods and volumes of treatment solution on biocementation were investigated. The results showed that the amount of carbonate precipitations increased with the dosage of treatment solution, providing cohesion for sand particles to resist wind erosion. At the same dosage, the spraying method tended to form a surface crust with higher calcium carbonate content but thinner thickness, offering the advantage of a lower initial wind erosion rate. The mixing method produced a homogeneous cementation across the treatment area, resulting in higher penetration resistance and slower wind erosion development. The combination treatment of spraying and mixing increased penetration resistance to 200 N and reduced wind erosion rate to almost $0 \text{ g·m}^{-2}\text{·min}^{-1}$, which is more effective in resisting persistent and intense wind erosion. This study determines the appropriate treatment method for SICP against wind erosion and its engineering application in the field.

Declarations

References

Ahenkorah I, Rahman MM, Karim MR, Teasdale PR (2020) A comparison of mechanical responses for microbial- and enzyme-induced cemented sand. Geotech Lett 10(4):559–567. https://doi.org/10.1680/jgele.20.00061

Almajed A, Tirkolaei HK, Kavazanjian E (2018) Baseline investigation on enzyme-induced calcium carbonate precipitation. J Geotech Geoenviron Eng 144(11):04018081. https://doi.org/10.1061/(ASCE)GT.1943-5606.0001973

Almajed A, Abbas H, Arab M, Alsabhan A, Hamid W, Al-Salloum Y (2020a) Enzyme-Induced Carbonate Precipitation (EICP)-Based methods for ecofriendly stabilization of different types of natural sands. J Clean Prod 274:122627. https://doi.org/10.1016/j.jclepro.2020.122627

Almajed A, Lemboye K, Arab GM, Alnuaim A (2020b) Mitigating wind erosion of sand using biopolymer-assisted EICP technique. Soils Found 60(2):356–371. https://doi.org/10.1016/j.sandf.2020.02.011

Alwalan M, Almajed A, Lemboye K, Alnuaim A (2023) Direct shear characteristics of enzymatically cemented sands. KSCE J Civ Eng 27(4):1512–1525. https://doi.org/10.1007/s12205-023-0817-2

ASTM D3080 (2012) Standard Test Method for Direct Shear Test of Soils Under Consolidated Drained Conditions. American Society for Testing and Materials, West Conshohocken, PA

Bagnold RA (1941) The physics of blown sand and desert dunes. Methuen, London, pp 64–69

Baziar MH, Sanaie M, Amirabadi OE (2021) Mitigation of dust emissions of silty sand induced by wind erosion using natural soybean biomaterial. Int J Civil Eng 19(5):595–606. https://doi.org/10.1007/s40999-020-00587-4

Chae SH, Chung H, Nam K (2021) Evaluation of Microbially Induced Calcite Precipitation (MICP) methods on different soil types for wind erosion control. Environ Eng Res 26(1):190507. https://doi.org/10.4491/eer.2019.507

Chung H, Kim SH, Nam K (2021) Application of microbially induced calcite precipitation to prevent soil loss by rainfall: effect of particle size and organic matter content. J Soils Sediments 21:2744–2754. https://doi.org/10.1007/s11368-020-02757-2

Dubey AA, Devrani R, Ravi K, Dhami NK, Mukherjee A, Sahoo L (2021) Experimental investigation to mitigate aeolian erosion via biocementation employed with a novel ureolytic soil isolate. Aeol Res 52:100727. https://doi.org/10.1016/j.aeolia.2021.100727

Dubey AA, Dhami NK, Ravi K, Mukherjee A (2023) Erosion mitigation with biocementation: a review on applications, challenges, & future perspectives. Rev Environ Sci Biotechnol 22(4):1059–1091. https://doi.org/10.1007/s11157-023-09674-z

Fattahi SM, Soroush A, Huang N (2020) Biocementation control of sand against wind erosion. J Geotech Geoenviron Eng 146(6):04020045. https://doi.org/10.1061/(ASCE)GT.1943-5606.0002268

Gao Y, He J, Tang X, Chu J (2019) Calcium carbonate precipitation catalyzed by soybean urease as an improvement method for fine-grained soil. Soils Found 59(5):1631–1637. https://doi.org/10.1016/j.sandf.2019.03.014

Gao Y, Hua C, Li Y, He J, Dai Z, Shen Y (2022) Biological solutions for the remediation of cracks in ancient earthen structures: Experimental studies. J Mater Civ Eng 34(11):04022312. https://doi.org/10.1061/(ASCE)MT.1943-5533.0004453

Ghasemi H, Hatam-Lee SM, Tirkolaei HK, Yazdani H (2022) Biocementation of soils of different surface chemistries via enzyme induced carbonate precipitation (EICP): An integrated laboratory and molecular dynamics study. Biophys Chem 284:106793. https://doi.org/10.1016/j.bpc.2022.106793

Hamdan NM, Kavazanjian EJr (2016) Enzyme-induced carbonate mineral precipitation for fugitive dust control. Géotechnique 66(7):546–555. https://doi.org/10.1680/jgeot.15.P.168

He J, Liu Y, Liu LX, Yan BY, Li LL, Meng H, Hang L, Qi YS, Wu M, Gao YF (2023) Recent development on optimization of biocementation for soil stabilization and wind erosion control. Biogeotechnics 1:100022. https://doi.org/10.1016/j.bgtech.2023.100022

Hoang T, Alleman J, Cetin B, Ikuma K, Choi SG (2019) Sand and silty-sand soil stabilization using bacterial enzyme induced calcite precipitation (BEICP). Can Geotech J 56(6):808–822. https://doi.org/10.1139/cgj-2018-0191

ISO (1984) Water quality: Determination of calcium content-EDTA titrimetric method. ISO 6058:1984. Geneva: ISO

Kok JF, Parteli EJ, Michaels TI, Karam DB (2012) The physics of wind-blown sand and dust. Rep Prog Phys 75(10):106901. https://doi.org/10.1088/0034-4885/75/10/106901

Li SH, Li CZ, Fu XL (2021) Characteristics of soil salt crust formed by mixing calcium chloride with sodium sulfate and the possibility of inhibiting wind-sand flow. Sci Rep 11:9746. https://doi.org/10.1038/s41598-021-89151-1

Lin H, Suleiman MT, Brown DG, Kavazanjian E (2016) Mechanical behavior of sands treated by microbially induced carbonate precipitation. J Geotech Geoenviron Eng 142(2):04015066. https://doi.org/10.1061/(ASCE)GT.1943-5606.0001383

Liu L, Gao Y, Geng W, Song J, Zhou Y, Li C (2023a) Comparison of jack bean and soybean crude ureases on surface stabilization of desert sand via enzyme-induced carbonate precipitation. Geoderma 435:116504. https://doi.org/10.1016/j.geoderma.2023.116504

Liu Y, Gao YF, He J, Zhou YD, Geng WJ (2023b) An experimental investigation on the erosion resistance of a soybean-urease induced carbonate precipitation cemented desert sand against the wind-induced erosion. Geoderma 429:116231. https://doi.org/10.1016/j.geoderma.2022.116231

Liu Y, Gao YF, Zhou YD, Meng H, Li C (2024) Evaluation of enzyme-induced carbonate precipitation using crude soybean urease during soil percolation. Acta Geotech 19(3):1571–1580. https://doi.org/10.1007/s11440-023-02040-x

Ma H, Zhou M, Hu Y, Hossain MS (2017) Interpretation of layer boundaries and shear strengths for stiff-soft-stiff clays using cone penetration test: LDFE analyses. Int J Geomech 17(9):06017011. https://doi.org/10.1061/(ASCE)GM.1943-5622.0000929

Maleki M, Ebrahimi S, Asadzadeh F, Tabrizi ME (2016) Performance of microbial-induced carbonate precipitation on wind erosion control of sandy soil. Int J Environ Sci Technol 13(3):937–944. https://doi.org/10.1007/s13762-015-0921-z

Meng H, Gao Y, He J, Qi YS, Hang L (2021) Microbially induced carbonate precipitation for wind erosion control of desert soil: field-scale tests. Geoderma 383:114723. https://doi.org/10.1016/j.geoderma.2020.114723

Mujah D, Shahin MA, Cheng L (2017) State-of-the-art review of biocementation by microbially induced calcite precipitation (MICP) for soil stabilization. Geomicrobiol J 34(6):524–537. https://doi.org/10.1080/01490451.2016.1225866

Ossai R, Rivera L, Bandini P (2020) Experimental study to determine an EICP application method feasible for field treatment for soil erosion control. Geo-Congress 2020: Biogeotechnics. American Society of Civil Engineers, Reston, VA, pp 205–213

Rice MA, Mullins CE, McEwan IK (1997) An analysis of soil crust strength in relation to potential abrasion by saltating particles. Earth Surf Proc Land 22(9):869–883

Sharaky AM, Mohamed NS, Elmashad ME, Shredah NM (2018) Application of microbial biocementation to improve the physico-mechanical properties of sandy soil. Constr Build Mater 190:861–869. https://doi.org/10.1016/j.conbuildmat.2018.09.159

Song J, Sim Y, Jang J, Hong W, Yun T (2020) Near-surface soil stabilization by enzyme-induced carbonate precipitation for fugitive dust suppression. Acta Geotech 15:1967–1980. https://doi.org/10.1007/s11440-019-00881-z

Sun XH, Miao LC, Wang HX, Wu LY, Zhang JZ (2021) Enzymatic calcification to solidify desert sands for sandstorm control. Clim Risk Manag 33:100323. https://doi.org/10.1016/j.crm.2021.100323

Wang Y, Sun XH, Miao LC, Wang HX, Wu LY, Shi WB, Kawasaki S (2024) State-of-the-art review of soil erosion control by MICP and EICP techniques: Problems, applications, and prospects. Sci Total Environ 912:169016. https://doi.org/10.1016/j.scitotenv.2023.169016

Whiffin VS, Van Paassen LA, Harkes MP (2007) Microbial carbonate precipitation as a soil improvement technique. Geomicrobiol J 24(5):417–423. https://doi.org/10.1080/01490450701436505

Woolley MA, van Paassen LV, Kavazanjian E (2020) Impact on surface hydraulic conductivity of EICP treatment for fugitive dust mitigation. Biogeotechnics 320:132–140. https://doi.org/10.1061/9780784482834.015

Xu J, Xiao Y, Xie GD, Wang YY, Zhen L, Zhang CS, Jiang Y (2020) Interregional ecosystem services benefits transfer from wind erosion control measures in Inner Mongolia. Environ Dev 34:100496. https://doi.org/10.1016/j.envdev.2020.100496

Zhang MX, Wang RQ, Liu FF, Xu P (2021) Anti-wind erosion and anti-dust mechanisms of microbial consolidation of bare soil. Environ Earth Sci 80(21):705. https://doi.org/10.1007/s12665-021-09977-w

Zomorodian SMA, Ghaffari H, O'Kelly BC (2019) Stabilization of crustal sand layer using biocementation technique for wind erosion control. Aeol Res 40:34–41. https://doi.org/10.1016/j.aeolia.2019.06

Zuniga-Barra H, Ortega-Martinez E, Toledo-Alarcon J, Torres-Aravena A, Jorquera L, Rivas M, Jeison D (2023) Potential use of microbially induced calcite precipitation for the biocementation of mine tailings. Minerals 13(4):506. https://doi.org/10.3390/min13040506